

Size Ratio of Fluvial Grains' Intermediate Axes Assessed by Image Processing and Square-Hole Sieving

Severin Stähly¹; Heide Friedrich²; and Martin Detert³

Abstract: The comparability of grain sizes emerging from different methods are discussed, including image-based grain-size analysis. Waterworked gravel-bed surfaces from laboratory and field experiments are analyzed in detail. Grain sizes estimated using freely available object-detection software are compared with grains measured with calipers by hand. On the basis of laboratory and field data, the pebble dimensions determined by square-hole sieving are demonstrated to underestimate real pebble dimensions by a factor of 0.83–0.86, and pebble dimensions derived from images underestimate the pebble-count measurements by a similar amount. Thus, for the present extensive data set, the software-detected grain sizes can be directly compared with grain sizes gained by square-hole sieving, as they are of the same order of magnitude. These results support future wide-spread use of image-based sieving for grain-size distribution analyses for both hydraulic research and engineering. DOI: [10.1061/\(ASCE\)HY.1943-7900.0001286](https://doi.org/10.1061/(ASCE)HY.1943-7900.0001286). © 2017 American Society of Civil Engineers.

Author keywords: Field measurement; Grain-size distribution; Gravel bed; Image processing; Object detection.

Introduction

Volumetric sampling and subsequent sieving is the classically applied method to determine a grain-size distribution (GSD). Because sieves with square holes are widely used, a combination of a grain's b -axis and c -axis determines whether the sieve opening size D retains the grain or not (Fig. 1), with the three principle body axes a , b , and c being the longest, intermediate, and shortest axis, respectively.

The geometric relation of mesh opening D to b and c is described by Church et al. (1987)

$$\frac{D}{b} = \frac{1}{\sqrt{2}} \left[1 + \left(\frac{c}{b} \right)^2 \right]^{0.5} \quad (1)$$

From infinitesimally flat to spherical particles, the ratio D/b ranges between 0.71 and 1, whereas for natural river beds, D/b typically is 0.79–0.82 (Graham et al. 2010). Thus, the results gained by square-hole sieving generally render a smaller value than the real length of the intermediate b -axis with the full length of the b -axis never being measured.

Classical laboratory sieving requires a demanding effort to classify sediments, and the process of digging, transporting, and sieving is time-consuming and cost-intensive. This holds true especially for coarse sediment mixtures, with the needed sampling volume typically governed by the maximum grain diameter. Alternatively, numerous in situ surface sampling methods have

been developed to obtain grading curves, especially for coarser sediment and a restricted sample size. Surface-sampling methods, such as pebble counts (e.g., Wolman 1954) or grid counts (e.g., Kellerhals 1971), are often used in field experiments. However, since digital cameras came onto the market, (semi)automatic image-based methods evolved as well (e.g., Maerz et al. 1996; Graham et al. 2005; Gislao 2009; Strom et al. 2010; ASTM 2010; Detert and Weitbrecht 2012; Kozakiewicz 2013). Image-based surface sampling takes little time in the field since one only takes a photo of the river bed. The ease of capturing photos with mobile devices and the increasing use of drones will likely make this a preferred method in GSD sampling in the future. Image-based screening allows the estimation of the surface-layer GSD without touching or disrupting the bed. Images taken from the bed can then be processed with (semi)automatic routines to yield GSDs. Typically, the routines identify particles within the image and then fit an ellipse with a long (a') and short (b') axis to the identified area of a particle. It is then assumed that these virtually seen axes correspond to the real longest (a) and intermediate (b) axis of a grain ($a' = a$ and $b' = b$). However, even if the error due to image processing can be neglected, the interaction between the grains leads to foreshortening, overlapping, and imbrication of grains (Graham et al. 2010). These effects may be amplified if the grain mixture has a large diversity in grain sizes and shapes. Fig. 2 gives a schematic sketch. Foreshortening would lead to $b > b' \geq c$, whereas burial and overlapping effects even could lead to $b' < c$. Consequently, $b > b'$ holds in every case. Graham et al. (2010) summarized that a data bias of b'/b typically falls between 0.80 and 0.99. This range of measured b'/b values is similar to the theoretical range of $D/b = 0.71 - 1$ for the difference between a particle's true b -axis and the corresponding opening of square-hole sieves.

Objective

Goal of this study is to quantify to what extent D/b and b'/b vary for typical fluvial river beds using the object-detection software *BASEGRAIN* (Detert and Weitbrecht 2012, 2013). Doing this is important for future applications of acquiring grain size

¹Ph.D. Student, Laboratory of Hydraulic Construction, EPF Lausanne, GC F1 485, CH-1015 Lausanne, Switzerland (corresponding author). E-mail: severin.staehly@epfl.ch

²Senior Lecturer, Dept. of Civil and Environmental Engineering, Univ. of Auckland, Private Bag 92019, Auckland, New Zealand. E-mail: h.friedrich@auckland.ac.nz

³Senior Assistant, Laboratory of Hydraulics, Hydrology and Glaciology, ETH Zurich, Hönggerberggring 26, HIA C11, CH-8093 Zürich, Switzerland. E-mail: detert@vaw.baug.ethz.ch

Note. This manuscript was submitted on March 3, 2016; approved on October 4, 2016; published online on February 9, 2017. Discussion period open until July 9, 2017; separate discussions must be submitted for individual papers. This technical note is part of the *Journal of Hydraulic Engineering*, © ASCE, ISSN 0733-9429.

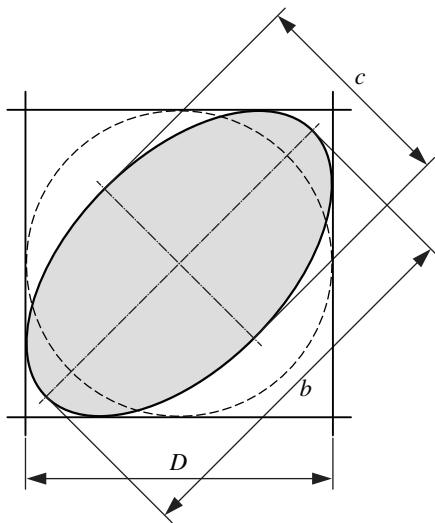


Fig. 1. Definition sketch for lengths D , b , and c , allowing for comparison between grain sizes determined by square-hole sieving and measured with caliper

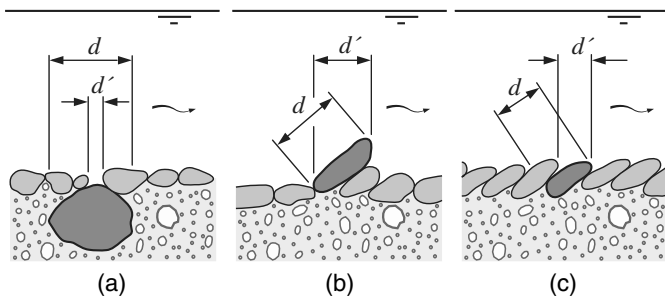


Fig. 2. Three potential causes for underestimating real grain sizes d as apparent grain size d' as object-detected on top-view photographs (redrawn from Graham et al. 2010, with permission from Wiley, copyright © 2000-2016 by John Wiley & Sons, Inc. or related companies, all rights reserved); grain size d is represented by intermediate b axis: (a) burial; (b) foreshortening; (c) overlapping (imbrication)

information using *BASEGRAIN* and other such related methods. New data sets of detailed measured grain sizes are presented, using extensive samples from laboratory and field, along with a comparison of quasi-square-hole sieving, line-sampling, and image-based methodologies.

Data Collection

Laboratory Data

Laboratory experiments were conducted in the Hydraulic Engineering Laboratory at the University of Auckland, New Zealand. The flume used was 19 m long, 0.45 m wide, 0.5 m deep, and set to a slope of 0.5%. The measurement area was located 14 m downstream of the inlet and consisted of a 1 m-long recess filled with gravel and leveled so that the gravel bed surface aligned with the surrounding channel bed. Artificial roughness was created by gluing grains on the channel bed upstream and downstream of the study site to achieve seemingly natural hydraulic conditions similar to these of the region of interest. To obtain a homogeneous illumination of the channel bed, neon lights were mounted at both flume sides. The photographs for the analysis with *BASEGRAIN*

were taken with a Nikon D5100 off-the-shelf camera (Tokyo) with 16 megapixels, fixed 0.6 m above the flume bed, typically resulting in resolution of about 0.14 mm/pixel (px). No distortion correction was applied.

The methods applied for grain sampling optimally work on a static waterworked layer, which in a first step needed to be created in the laboratory channel. The channel bed was waterworked with a slowly rising discharge up to 0.067 m³/s. As a criterion for a static waterworked layer, the sediment transport was measured at the downstream end of the flume. When a value close to zero was observed during multiple hours, the water in the flume was drained and the flume bed was dried for the upcoming photo documentation, which enables derivation of the grains' apparent a' -axis and b' -axis by image analysis. This procedure was conducted twice (Experiments I and II). The b -axis and c -axis of the grains were inventoried manually along transects (Fehr 1987a, b) to be able to derive a related mesh opening D by applying Eq. (1).

Field Data

About 500 grains have been measured manually at each of three study sites: Tairua River (S 37.069; E 175.767), Whakatiwai I (S 37.087; E 175.301) and Whakatiwai II (S 37.088; E 175.299). These two first-order rivers are located in the North Island of New Zealand. Whakatiwai River is a small ungauged creek with an estimated average discharge of 0.1–1 m³/s and a bed slope of 1.5–2%. Tairua River is larger, with an average discharge of 1–10 m³/s and a bed slope of 0.1–0.2%. Surface structures were documented by top-view photos with the same camera as used during the laboratory experiments. Photos were taken in handheld mode from a height of about 1.5–2.0 m, resulting in typical resolutions of about 0.35–0.5 mm/px. The b -axis and c -axis of the grains were inventoried manually along transects (Fehr 1987a, b), in line with the laboratory procedure.

Analysis Methodology

Line-Sampling

The analysis of samplings along transects according to Fehr (1987a, b) is commonly used for alpine gravel-bed rivers to estimate the GSD of both the surface and subsurface layers. All grains lying along the projection of a thread, which was fixed across the area of interest, are sampled. In a field protocol, all b -axes larger than a threshold value are inventoried to their correct size class. For the current study, both in the laboratory as well as in the field, three line-samplings were taken on every sampling site to collect representative data. The grains were measured always by the same person using a caliper. The lower limit was set to 5 mm. The caliper restricted the accuracy to 0.5 mm.

The methodology by Fehr (1987a, b) allows the conversion of a transect-by-number count of a waterworked surface layer to a volume-by-weight distribution of the subsurface layer based on semiempirical equations. However, in the current study, no conversion to a volume-by-weight distribution was considered nor applied, as the focus of this study is on grain sizes and not on GSDs.

BASEGRAIN

BASEGRAIN is a free tool for semiautomatic sediment-grain detection and the analysis of the grains' geometry. An example screenshot is given in Fig. 3. *BASEGRAIN*'s functions relevant to this study will now be briefly explained. Detailed information

on the methodology and the functions of the program are provided by Detert and Weitbrecht (2012, 2013).

The starting point for *BASEGRAIN* is an image showing a representative section of a river bed in top-view perspective. Then, the section in the image used for the analysis, as well as the image scale (reference distance, e.g., ruler or known flume width) must be selected. After determination of the optimal parameters' set for the automated image processing techniques, *BASEGRAIN* identifies the top-view area of all grains visible on the image. The particle separation process consists of five steps. In the first three steps, the interstices are detected by different methods using a grayscale threshold approach, a bottom-hat transformation technique, and gradient filters. In Step 4, a watershed algorithm is applied. Here, the focus changes from detection of interstices to the separation of single-grain areas, resulting in a binary image with fully-confirmed single-grain elements. In the final step, the region properties of each grains' top-view area are obtained. Erroneous particle separation can be corrected individually using the manual postprocessing tools (Fig. 3). The software then replaces each particle area with an ellipse of the same normalized second central moment to obtain an estimate to the biased a' -axis and b' -axis. *BASEGRAIN* allows the estimation of the volumetric GSD of the subsurface layer according to the method after Fehr (1987a, b) based on the determined b' -axes weighted by number. However, the current study only considers the statistics by number and not by volume.

During the laboratory experiments, photographs of the waterworked flume bed were taken for both with and without

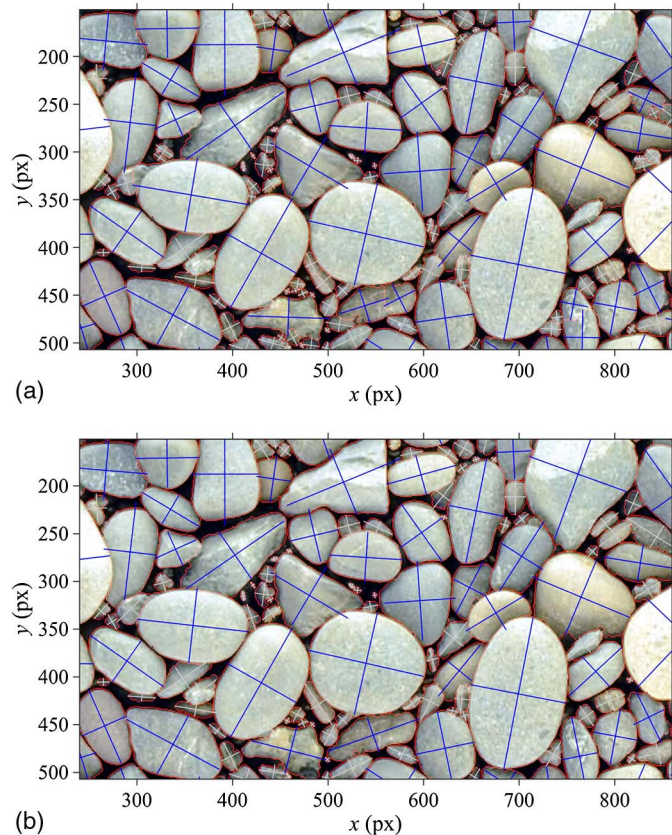


Fig. 3. Typical snapshot result of *BASEGRAIN*: (a) before; and (b) after using the manual postprocessing tools; image shows a part of water-worked laboratory flume bed of $356 \times 620 \text{ px}^2 = 60 \times 105 \text{ mm}^2$; only grains with a' -axes and b' -axes highlighted in blue (here $b' > 5 \text{ mm} = 29.6 \text{ px}$) are considered in the analysis, while white axes indicate that sizes fall below truncation criterion (here, $b' \leq 5 \text{ mm}$)

the thread used for the line sampling in the image. This allowed the direct comparison of the results obtained by *BASEGRAIN* with those obtained by manual line-sampling. Unfortunately, this procedure was not feasible during the field experiments.

Results

Square-Hole Sieve Correction Factor (D/b Ratio) for Flume Data Set

In total, the b -axes and c -axes of 738 grains were collected and measured by hand in the two laboratory experiments. As shown in Fig. 4, the results of the square hole sieve correction factor D/b [calculated via b -axis and c -axis, Eq. (1)] have a large scatter in both experiments that fall between the theoretical minimum and maximum value of 0.71 and 1 (Table 1).

Despite this large variation within each data set, the median of D/b lies at 0.83–0.84 and does not vary significantly between the two different experiments, indicating that a statistically meaningful number of grains had been measured. The standard deviation of D/b is almost constant with values of 0.055.

Intermediate Axis Correction Factor (b'/b Ratio) for Flume Data Set

Since the GSDs measured by line-sampling during the two laboratory experiments were almost identical, one data set of pebbles was used to determine an averaged b'/b ratio that fits the data set best; the other data set was used to validate this result.

First, the b -axes intervals measured by both manual sampling and *BASEGRAIN* were compared, and the corresponding b'/b ratio was computed. For this reason, a photo of the waterworked flume bed with the thread for the line-sampling was taken. Experiment II was chosen, totaling 202 grains for which b and b' have been

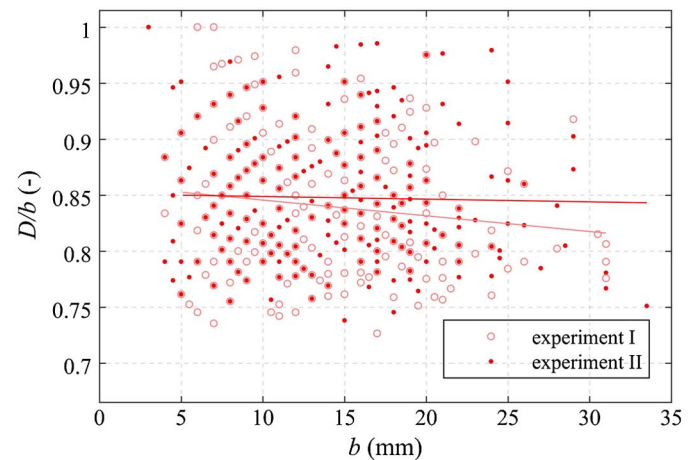


Fig. 4. Sieve correction factor D/b [Eq. (1)] for line-samplings of laboratory Experiments I and II; linear fits to data sets indicate a slight decrease of D/b towards larger grain sizes

Table 1. Data Obtained by Hand Measurement from the Two Laboratory Experiments

Item	Unit	Experiment I	Experiment II
Number of stones	(—)	393	345
D/b	(—)	0.833 ± 0.055	0.839 ± 0.055

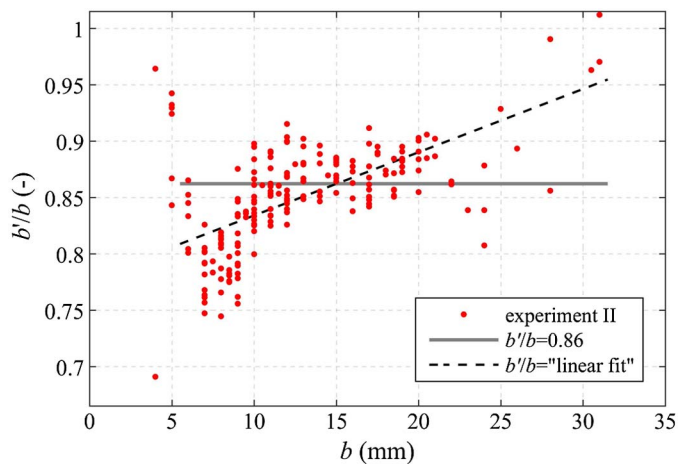


Fig. 5. Underestimation of real grain sizes b inventoried by line-sampling against grain sizes b' measured by *BASEGRAIN*, both determined during Experiment II

determined pairwise for each grain both using *BASEGRAIN* and the calipers.

In Fig. 5 b'/b is plotted against b . The data show a large scatter with a slightly increasing tendency towards larger b . Thus, the largest *BASEGRAIN*-detected b' -axes appear to be less affected by burial, overlapping, and foreshortening than the smaller grain sizes. Calibration, by using the least-squares method, results in a constant ratio of $b'/b = 0.86$. A linear fit from 0.78 to 0.95 for zero to a maximal b provides a slightly better match, especially for larger grains. The large scatter of b'/b for $b \leq 5$ mm is most likely caused by two effects: (1) the insufficient precision of the b -axes measured, as the caliper used measurements restricted to the nearest 0.5 mm and (2) for the sediment mixture used small and flat grains ($b \gg c$) had a larger tendency to be subjected to overlapping, foreshortening and burial compared to larger grains, resulting in small grains tending not to show their b -axis on the surface. Thus, the bias due to discretization is then $<10\%$. Furthermore, b -axes < 5 mm here correspond to sizes of about ~ 35 px, what is above the limit

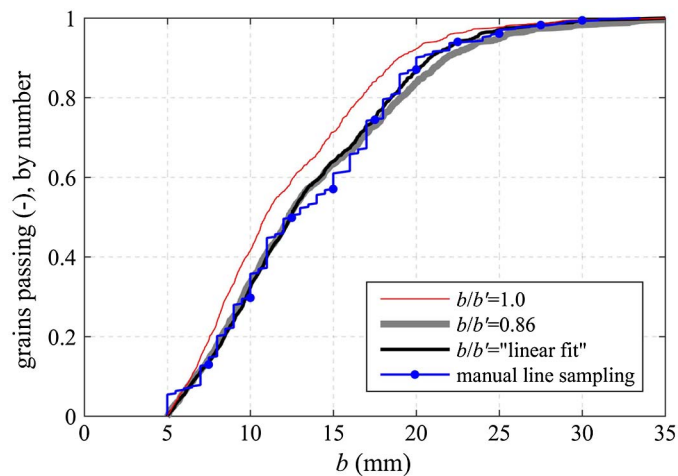


Fig. 6. GSDs (b -axis of grains passing by number along transects) of stones collected in Experiment I (345 grains) and *BASEGRAIN* analysis (1,578 grains for $b/b' = 1.0$, and 1,757 grains for $b/b' = 0.86$, and 1,799 grains for linear fit, respectively; a higher number of the two latter is due to truncation at $b < 5$ mm, but $b \neq b'$)

Table 2. Results for D/b Obtained at Three Field Measurement Sites at Two Rivers

Item	Unit	Tairua River	Whakatiwai I	Whakatiwai II
Number of stones	(—)	498	509	500
D/b	(—)	0.863 ± 0.064	0.850 ± 0.059	0.833 ± 0.064

of 23 px as proposed by Graham et al. (2005) for their object-detection method, which is similar to that applied by *BASEGRAIN*. Thus, the scatter due to misleading image processing is supposed to be low. Nevertheless, every time an additional unknown bias due to imperfect determination of b' is introduced by the image processing of *BASEGRAIN* as well. Consequently, Fig. 5 depicts the measured relation of b and b' influenced by the integral over several biases.

To validate that $b'/b = 0.86$, the ratio was applied to the data of Experiment I. Since identical conditions (discharge, sediment mixture, and flume) were used to create the subsurface layer, it was assumed that the parameters gained from Experiment II will help to provide a proper fit. Fig. 6 shows that without applying any correction factor ($b'/b = 1.0$), the *BASEGRAIN*-detected grain sizes generally underestimate these obtained manually. Furthermore, the object-detected grains were scaled up by $b'/b = 0.86$, showing an adequate fit. However, the curves still slightly differ. The linear fit found for the data set of Experiment II further improves the matching of the curves especially for larger grains, here for $b > 17$ mm.

Square-Hole Sieve Correction Factor (D/b Ratio) for Field Data Set

Field experiments with respect to the D/b ratio were conducted to evidence the differences between laboratory and field data. The average D/b ratio was determined to 0.83–0.85 at Whakatiwai River, while the sample from Tairua River was at 0.86 (Table 2 and Fig. 7). The standard deviation does not differ significantly between the sites and the different rivers, with values varying between 0.059 and 0.064, i.e., only slightly higher than observations from the laboratory experiments (compare with Table 1).

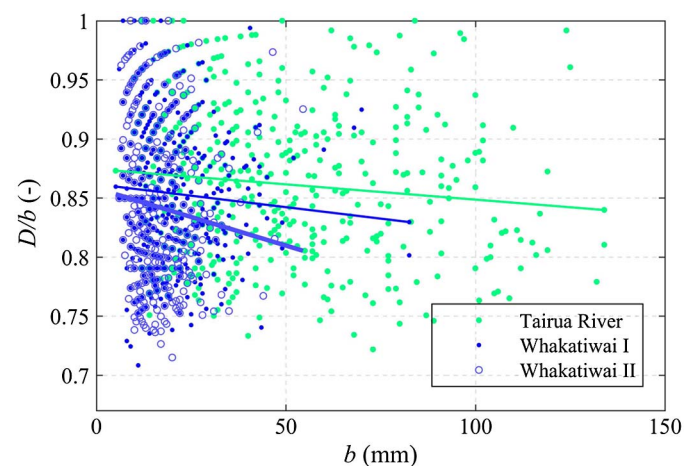


Fig. 7. Sieve correction factor D/b [Eq. (1)] obtained at three field sites; lines show linear fits to data sets; apparent pattern for smaller b values is due to its discretization to a multiple of 0.5 mm

Discussion

The medians of all D/b ratios determined during this study lie between 0.83 and 0.86 for both laboratory and field experiments. This is surprising since the conditions, including mixture composition, flow discharge, bed stress, etc., differed substantially between laboratory tests and field sites. In the laboratory, a constant discharge and water depth was applied, resulting in a temporarily constant shear force. The surface layer of the laboratory study is therefore more uniform than found in the natural environment. In general, the D/b ratio depends on the grains' shapes, which in turn depend mainly on the sediment mixture used in the laboratory and on the transported distance in the field (Bunte and Abt 2001). The D/b ratio appears to be rather insensitive to different environments, as already stated by Graham et al. (2005). However, they found average D/b ratios of 0.79–0.82 for their three field sites tested. The values of 0.83–0.86 from the present study are slightly higher. This discrepancy appears to be caused by different granulometric site properties. However, different grain-selection methods used in the two studies may also contribute to deviations. The D/b ratios obtained in the present study were determined from 2,245 (1,507 field and 738 laboratory) single grains collected manually from the surface layer along transects, and their dimensions were recorded to the nearest 0.5 mm, whereas Graham et al. (2005) selected 500 clasts at three study sites (1,500 cobbles in total) and recorded their dimensions to the nearest 5 mm.

Both laboratory and field experiments in the present study have shown that the D/b ratios of the different grains vary strongly within the same grain size. Applying a single value, therefore, does not give a perfect solution. However, since the average value turned out to be more or less constant for all measuring sites, applying a constant D/b ratio of about 0.83–0.86 provides better results than applying no factor at all.

The b'/b ratio was expected to be lower than 1 due to imbrication, foreshortening, and burial. A constant b'/b of about 0.86 was found. Alternatively to 0.86, a linear fit from 0.78 to 0.95 from zero to the maximum b improves matching the real size of the coarse-grain fraction. Consequently, the D/b' ratio computed from the found ratios of D/b and b'/b is around 1, indicating that D/b and b'/b ratios almost cancel each other. Thus, BASEGRAIN-detected grain sizes b' are directly comparable with the results of screen-meshed D by square-hole sieves.

Conclusions

This study's findings of D/b of approximately 0.83–0.86, b'/b of approximately 0.86, and, consequently, D/b' of approximately 1, are based on a nonoverarching data set involving gravel beds from laboratory flume and two different rivers. Future research, focusing on size-class-dependent b'/b , would further improve the knowledge on how particle size relates to burial, overlapping, and foreshortening, which continues to be a major challenge for image-based screening methods. Obtaining data from other locations, including grains with substantially different shape and size characteristics, will allow a database to be built up that supports widespread application, as well as classification. It can be expected that future testing of the b'/b value in field environments will lead to improvement and diversification of the ratio needed as an input for image-based GSD calculations.

Acknowledgments

The financial support of the Master's thesis of the first author by the Zeno Karl Schindler Foundation, Geneva and the Erich Degen Foundation, Zurich (#201428) is gratefully acknowledged. The authors would like to thank S. Bertin, for assistance in acquiring the data. H. Friedrich is supported by the Marsden Fund (Grant No. UOA1412), administered by the Royal Society of New Zealand.

Notation

The following symbols are used in this paper:

- a = grain's a -axis (mm);
- b = grain's true b -axis (mm);
- b' = projection of the seen b on photograph (mm);
- c = grain's c -axis (mm);
- c' = projection of the seen c on photograph (mm);
- D = square-hole sieve opening (mm); and
- d = grain diameter (mm).

References

- ASTM. (2010). "Standard test methods for determining average grain size using semiautomatic and automatic image analysis." *ASTM E1382-97*, West Conshohocken, PA.
- BASEGRAIN version 2.1 [Computer software]. ETH Zurich, Zürich, Switzerland.
- Bunte, K., and Abt, S. R. (2001). "Sampling surface and subsurface particle-size distributions in wadable gravel- and cobble-bed streams for analyses in sediment transport, hydraulics, and streambed monitoring." *General Technical Rep. RMRS-GTR-74*, Dept. of Agriculture, Forest Service, Rocky Mountain Research Station, Fort Collins, CO.
- Church, M. A., McLean, D. G., and Wolcott, J. F. (1987). "River bed gravels: Sampling and analysis." *Sediment transport in gravel-bed rivers*, C. R. Thorne, J. C. Bathurst, and R. D. Hey, eds., Wiley, Chichester, U.K., 43–88.
- Detert, M., and Weitbrecht, V. (2012). "Automatic object detection to analyze the geometry of gravel grains: A free stand-alone tool." *River flow 2012*, R. M. Muñoz, ed., Taylor & Francis, London, 595–600.
- Detert, M., and Weitbrecht, V. (2013). "User guide to gravelometric image analysis by BASEGRAIN." *Advances in science and research*, S. Fukuoka, H. Nakagawa, T. Sumi, and H. Zhang, eds., Taylor & Francis, London, 1789–1795.
- Fehr, R. (1987a). "Einfache Bestimmung der Korngrößenverteilung von Geschiebematerial mit Hilfe der Linienzahlanalyse [Simple detection of grain size distribution of sediment material using line-by-number analysis]." *Schweizer Ingenieur und Architekt*, 105(38), 1104–1109 (in German).
- Fehr, R. (1987b). "Geschiebeanalysen in Gebirgsflüssen [Grain size analyses in torrents]." *Rep. No. 92*, Laboratory of Hydraulics, Hydrology and Glaciology (VAW), ETH Zurich, Zurich, Switzerland (in German).
- Gislao, M. (2009). "Performing a grains analysis in 5 easy steps." (http://www.olympusamerica.com/seg_industrial/files/Grains123_092509.pdf) (Dec. 23, 2015).
- Graham, D. J., Rice, S. P., and Reid, I. (2005). "A transferable method for the automated grain sizing of river gravels." *Water Resour. Res.*, 41(7), 1–12.
- Graham, D. J., Rollet, A.-J., Piégay, H., and Rice, S. P. (2010). "Maximizing the accuracy of image-based surface sediment sampling techniques." *Water Resour. Res.*, 46(2), 1–15.
- Kellerhals, R., and Bray, D. I. (1971). "Sampling procedures for coarse fluvial sediments." *J. Hydraul. Div.*, 97, 1165–1180.

Kozakiewicz, J. (2013). "Automated image analysis for measuring size and shape of Martian sands." (<http://www.lpi.usra.edu/meetings/lpsc2013/programAbstracts/view/>) (Dec. 23, 2015).

Maerz, N. H., Palangio, T. C., and Franklin, J. A. (1996). "WipFrag image based granulometry system." *Proc., FRAGBLAST 5 Workshop on Measurement of Blast Fragmentation*, A.A. Balkema, Montréal, 91–99.

Strom, K. B., Kuhns, R. D., and Lucas, H. J. (2010). "Comparison of automated image-based grain sizing to standard pebble-count methods." *J. Hydraul. Eng.*, 10.1061/(ASCE)HY.1943-7900.0000198, 461–473.

Wolman, M. (1954). "A method of sampling coarse river-bed material." *Trans. Am. Geophys. Union*, 35(6), 951–956.